State-Resolved Gas-Surface Reactivity of Methane in the Symmetric C-H Stretch Vibration on Ni(100)

Plinio Maroni, Dimitrios C. Papageorgopoulos, Marco Sacchi, Tung T. Dang, Rainer D. Beck,* and Thomas R. Rizzo
Laboratoire de Chimie Physique Moleculaire, École Polytechnique Fédérale de Lausanne, CH-1015 Lausanne, Switzerland
(Received 23 February 2005; published 22 June 2005)

The state-resolved reactivity of CH_4 in its totally symmetric C-H stretch vibration (ν_1) has been measured on a Ni(100) surface. Methane molecules were accelerated to kinetic energies of 49 and 63.5 kJ/mol in a molecular beam and vibrationally excited to ν_1 by stimulated Raman pumping before surface impact at normal incidence. The reactivity of the symmetric-stretch excited CH_4 is about an order of magnitude higher than that of methane excited to the antisymmetric stretch (ν_3) reported by Juurlink *et al.* [Phys. Rev. Lett. **83**, 868 (1999)] and is similar to that we have previously observed for the excitation of the first overtone ($2\nu_3$). The difference between the state-resolved reactivity for ν_1 and ν_3 is consistent with predictions of a vibrationally adiabatic model of the methane reaction dynamics and indicates that statistical models cannot correctly describe the chemisorption of CH_4 on nickel.

DOI: 10.1103/PhysRevLett.94.246104 PACS numbers: 82.65.+r, 34.50.Rk, 68.35.Ja, 68.43.-h

Activated dissociation of molecules on a metal surface is a fundamental step in many catalytic processes. An important example is the chemisorption of methane on nickel to form surface-bound methyl and hydrogen; this reaction is the rate-limiting step in steam reforming, which is the principal process for industrial hydrogen production. The importance of this process has incited a number of studies, both theoretical and experimental, directed towards understanding the detailed mechanism of methane chemisorption [1–15]. Molecular-beam experiments have shown that methane chemisorption on nickel is a direct process, activated by translational and vibrational energy [1,2]. More recent state-resolved experiments investigating the reactivity of CH_4 excited to the antisymmetric stretch fundamental vibration (ν_3) [6] and first overtone ($2\nu_3$) [9] on Ni(100) have found that energy in ν_3 promotes the reaction with similar efficacy as kinetic energy along the surface normal. Furthermore, Juurlink *et al.* [6] have shown that CH_4 with excitation in ν_3 contributes less than 2% to the activated chemisorption of thermally excited methane [2]. They conclude that vibrational modes other than ν_3 must play a significant role in methane reactivity under thermal conditions. Theoretical treatments of methane chemisorption include statistical [11,12] as well as dynamical models [3,4,7,8,13]. While the statistical approach excludes the possibility of mode-specific reactivity, it has been claimed to reproduce the results of both thermally averaged and eigenstate-resolved measurements for CH_4 on Ni(100) [11,12]. On the other hand, simplified dynamical models for gas-surface reactions suggest the possibility of mode specificity [7,8]. For reactions that occur entirely in the gas phase, more realistic dynamical calculations find that the symmetric-stretch vibration is generally more efficient than the antisymmetric stretch in promoting reaction [16–22], and this has been confirmed, in part, by experiments [18,23].

We have previously reported vibrational mode-specific chemisorption of CD_2H_2 on Ni(100), where we demonstrated the difference in reactivity of two nearly isoenergetic overtone levels [10]. Directly testing the prediction of higher reactivity for the symmetric stretch relative to the antisymmetric stretch in methane is more challenging, however, since direct IR excitation cannot be used to excite CH_4 via totally symmetric vibrations such as ν_1. We report here the first use of stimulated Raman pumping (SRP) to measure the state-resolved surface reactivity of $CH_4(\nu_1)$ on Ni(100). Both SRP and IR excitation have been used previously [24] to study the gas-phase reaction of CH_4 with chlorine atoms to compare the effects of ν_1 and ν_3 excitations on the dynamics. While no significant difference was observed in the rovibrational product state and angular distributions for the two states, the study did not exclude the possibility of different reaction cross sections.

Our state-resolved sticking coefficient measurements are performed in a molecular-beam/surface science apparatus designed to study the interaction of laser-excited molecules with single crystal surfaces. Only the key aspects of this setup are reported here; details can be found in Ref. [14]. A triply differentially pumped molecular-beam source produces gas pulses of 27 μs duration at a repetition rate of 20 Hz. These pulses, consisting of methane seeded in hydrogen, enter an ultrahigh vacuum (UHV) surface science chamber where they collide with a 10 mm diameter Ni(100) single crystal surface at normal incidence. We use time-of-flight measurements to determine the kinetic energy of the methane molecules incident on the surface. We determine the methane rotational temperature to be less than 10 K by cavity ring-down spectroscopy in a separate chamber with an identical molecular-beam valve.

A fraction of the incident methane molecules are prepared in the ν_1 state by SRP starting from the $J = 0$, 1, and 2 rotational levels, which represent the ground states of the three nuclear spin species of CH_4. Because the Raman pumping process is not particularly efficient, intense pulsed laser beams are needed to saturate the transitions.

The optical layout used to produce the required laser frequencies is shown in Fig. 1.

The 532 nm Raman pump beam is produced by generating the second harmonic of an injection-seeded, Nd:YAG laser operating at 20 Hz. The Stokes radiation at 630 nm is generated by a dye laser and amplified in a methane-filled Raman amplifier, both of which are pumped by the same Nd:YAG laser. To avoid beam instabilities resulting from thermal lensing inside the Raman amplifier, the methane is continuously circulated by a series of fans. Both the pump and Stokes beams entering the UHV chamber each have energies of 250 mJ/pulse. The methane pressure of 9 bar in the Raman amplifier is chosen to tune the maximum of the gain profile to overlap the $Q(0)$, $Q(1)$, and $Q(2)$ transitions used to excite the methane molecules in the molecular beam. Since the 0.05 cm^{-1} bandwidth of the Stokes radiation is insufficient to resolve these transitions, which have Raman shifts of 2916.47, 2916.49, and 2916.53 cm^{-1}, respectively [25], we assume in our analysis that Raman excitation takes place simultaneously on all three transitions. Pump and Stokes laser beams were focused on a 1.6 mm (FWHM) long line parallel to the molecular beam by a cylindrical lens ($f = 300$ mm) as shown in Fig. 2. A CCD beam profiler monitors the overlap of the pump and Stokes beams and determines the respective focal widths to be 41 ± 3 and 52 ± 4 μm.

To perform state-resolved gas-surface reactivity measurements, we expose the Ni(100) surface to the laser-excited molecular beam for a predetermined time while monitoring the CH_4 flux with a calibrated quadrupole mass spectrometer. The sample surface is heated to 473 K throughout the deposition in order to keep the surface free of adsorbed hydrogen. After the deposition, we detect the carbon produced by CH_4 chemisorption using Auger electron spectroscopy (AES). The Auger signal is calibrated in terms of carbon coverage using the self-limiting adsorption of 0.5 ML carbon on Ni(100) resulting from a saturation exposure of methane or ethylene. The Auger measurements are repeated for different positions across the sample surface, producing the carbon profile shown in Fig. 2. The tight focusing of the laser beams within the molecular beam generates several distinct regions within this profile. The narrow peak in the center is due to the reaction of both laser-excited (''laser-on'') and unexcited (''laser-off'') CH_4 molecules. The broad shoulders on either sides of this peak represent the carbon footprint of the molecular beam ($\varnothing = 1.7$ mm) due to chemisorption of unexcited CH_4. The carbon signal outside the molecular-beam footprint is due to carbon adsorbed from the background pressure in the chamber (3×10^{-10} mbar) during the 90 min deposition time. The rise in the carbon baseline is due to the electron beam induced carbon formation during the 30 min Auger analysis. For the calculation of the state-resolved reactivity, we subtract an extrapolated laser-off baseline from the central peak and integrate the resulting laser-on carbon peak along the z direction. The width of this peak is significantly larger than the width of laser focus along the z direction. This difference results from angular misalignment between the laser focal lines and the molecular beam, the finite size of the Auger electron beam (FWHM = 140 μm) and the spatial jitter of the two laser beams along the z direction. Because of the broadening, we use the C/Ni AES peak integral rather than peak height in our analysis of the state-resolved sticking coefficient.

The number of excited molecules incident on the surface is determined from the molecular-beam flux, the laser focal volume, and the saturation parameter of the Raman transition. The latter is determined by fitting a numerical model of the Raman excitation process, including the laser beam profiles, to the fluence dependence of the laser-on carbon

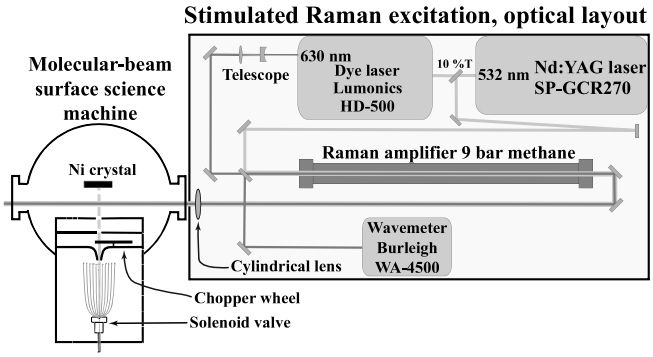

FIG. 1. Optical setup used for stimulated Raman pumping of CH_4 in the molecular beam.

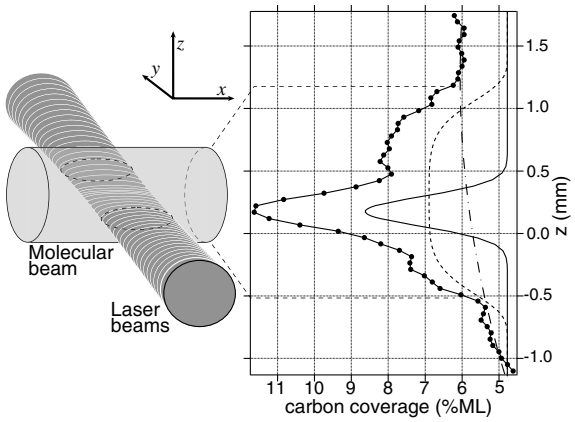

FIG. 2. Auger analysis of deposited carbon (right-hand side) together with a schematic of the excitation region (left-hand side). The individual contributions to the carbon signal from the electron beam induced carbon formation during the Auger analysis (dash-dotted line), the unexcited molecular beam (dashed line) and the laser-excited beam (solid line) are shown separately. These data were obtained at a molecular-beam kinetic energy of 63.5 kJ/mol with laser energies of 250 mJ/pulse for both the pump and the Stokes radiation.

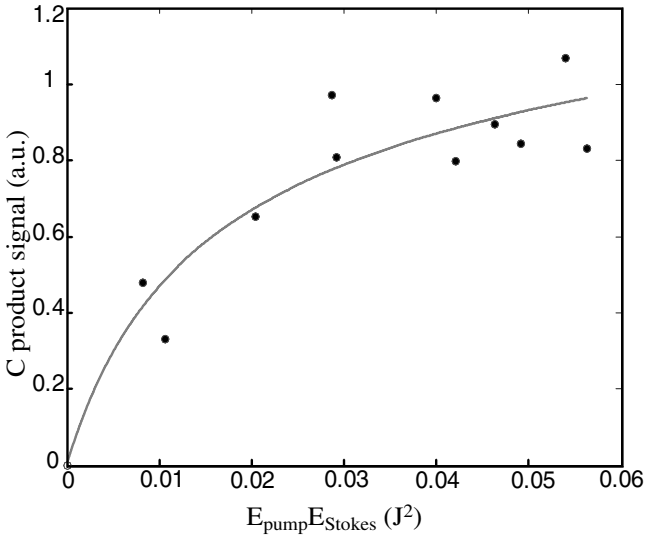

FIG. 3. Fluence dependence of laser-on carbon signal produced by chemisorption of $CH_4(\nu_1)$.

signal (Fig. 3). We excite 0.1% of the $(1.01 \pm 0.02) \times 10^{14}$ molecules/(cm^2 s) that impinge on the surface.

The state-resolved sticking coefficient $S_0(\nu_1)$ obtained from the ratio between the integrated carbon signal and the incident dose of $CH_4(\nu_1)$ is shown in Fig. 4 for 49 and 63.5 kJ/mol of translational energy. For comparison, we show state-resolved sticking coefficients for the antisymmetric stretch, $S_0(\nu_3)$, reported by Juurlink *et al.* [5,6], as well as our previous measurements [9] of $S_0(2\nu_3)$ and of S_0 (laser-off). Experimental limitations prevented us from measuring $S_0(\nu_1)$ at higher and lower kinetic energies: for the higher kinetic energies, the difference in reaction probability between unexcited and laser-excited molecules

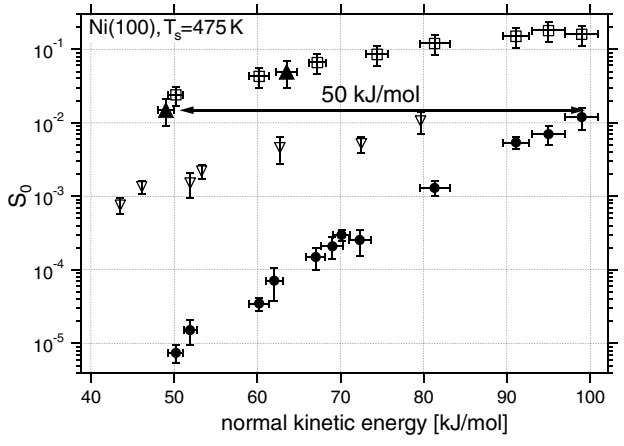

FIG. 4. State-resolved sticking coefficients for CH_4 in the ν_1 (▲), $2\nu_3$ (□) [9], ν_3 (▽) [5], and ground (●) [9] vibrational states on Ni(100) as a function of incident kinetic energy normal to the surface. The error bars represent the 95% confidence interval of the convoluted uncertainties. The major source of uncertainty comes from our estimation of the focal volume.

decreases rapidly, making the laser-on peak too difficult to detect above the laser-off background; for lower kinetic energy, the reactivity of the laser-excited beam is too low to produce a detectable carbon signal above that from the residual gas in the chamber.

For the two kinetic energies investigated, we found $S_0(\nu_1)$ to be almost equal to $S_0(2\nu_3)$ measured previously with our setup using IR overtone excitation [9], despite the fact that the former has half the amount of vibrational energy. Moreover, comparison of our results for $S_0(\nu_1)$ with those for $S_0(\nu_3)$ obtained by Juurlink *et al.* [5,6] shows that excitation of CH_4 to the symmetric stretch (ν_1) increases the reactivity approximately 10 times more than excitation to the antisymmetric stretch (ν_3). Such a large difference in reactivity between two nearly isoenergetic states is a clear sign of mode-specific chemisorption of CH_4 on Ni(100) and is totally inconsistent with a statistical description of the reaction [11,12]. We have previously observed vibrational mode specificity in the reaction of CD_2H_2 on Ni(100), where excitation of the combination band ($\nu_1 + \nu_6$) containing one quantum each of symmetric and antisymmetric CH stretch vibration increases reactivity up to 5 times more than the antisymmetric stretch overtone ($2\nu_6$) [10]. In this case, the difference in reactivity for the two isoenergetic states of CD_2H_2 could be rationalized by the different vibrational amplitudes of the two CH bonds for the initially prepared quantum states. This is consistent with a number of gas-phase examples of bond-specific chemistry where the reactivity of a bond is directly related to its amount of stretch excitation [26,27].

For CH_4, the observed difference in reactivity between ν_1 and ν_3 cannot be explained simply in terms of bond-specific laser excitation, since all four CH bonds initially carry amplitude for both states. However, recent theoretical models based on a vibrationally adiabatic treatment [8,16,19–22] suggest that the interaction with the approaching reaction partner can lead to energy localization which is different for different initial states, resulting in mode-specific reactivity, and this has been confirmed by experimental results in gas-phase reactions [18,23]. Halonen *et al.* [8] used this vibrationally adiabatic model to simulate the interaction of a vibrating CH_4 molecule close to a flat nickel surface. They predict that the vibrational energy of the symmetric and antisymmetric stretches becomes localized in the proximal and distal CH bonds, respectively, during the adiabatic approach toward the surface, and based on this they suggest that $CH_4(\nu_1)$ should be significantly more reactive than $CH_4(\nu_3)$ in the adiabatic limit. In calculations for gas-phase reactions [16,17,19–22], similar vibrational adiabatic models are used to investigate the reactivity of vibrationally excited molecules. All these calculations show that the symmetric stretch of the reactant transforms adiabatically into the stretching of the bond that breaks during the reaction. In

fact, Halonen *et al.* suggested that the experimentally observed increase in reactivity for CH_4 upon excitation of ν_3 is due to curve crossing to the reactive ν_1 state at incident speed above the Massey velocity [8]. The large difference between $S_0(\nu_1)$ and $S_0(\nu_3)$ that we observe would indicate that the mixing due to the curve crossing is far from complete at the kinetic energies of our experiment. Although the predictive capabilities of the vibrationally adiabatic model alone may be limited due to its strongly simplifying assumptions, it is reinforced by the experimental observation of a large difference in reactivity for the symmetric and antisymmetric stretch vibrations. Moreover, the experimentally confirmed prediction of the vibrationally adiabatic model should encourage efforts to develop more sophisticated dynamical treatments of methane chemisorption. On the other hand, our results are clearly inconsistent with statistical theories, which assume rapid intramolecular energy randomization and predict reactivities that scale with total internal energy independent of the initially excited vibrational state.

Using a different approach than vibrationally adiabatic models previously cited, Milot *et al.* [7] have performed wave packet calculations of methane scattered from a flat surface, including all nine internal vibrations. Based on the calculated kinetic energy loss during the collision, they predicted the same trend in reactivity: $\nu_1 > \nu_3 > \nu_4 >$ ground state.

In addition to comparing the effect of different vibrational modes on the reactivity of methane on nickel, we can compare the effect of vibrational energy in ν_1 with that of translational energy. One can see from Fig. 4 that putting 35 kJ/mol of vibrational energy in ν_1 results in the same increase in reactivity as adding 50 kJ/mol of kinetic energy normal to the surface. This indicates that energy in ν_1 is 1.4 times more efficient than translational energy in promoting the reaction. A similar effect has been observed for $CH_4(\nu_3)$ on Ni(111) [15], where the relative efficacy of ν_3 was found to be 1.25 compared to translational energy. Smith *et al.* have argued that an efficacy larger than 1 can result either from lattice recoil, where some translational energy is lost to the motion of the surface [3], or from nonadiabatic dynamics, where ground state molecules do not follow the minimum energy path due to coupling between translation and vibration [15].

In conclusion, we have used stimulated Raman pumping to measure for the first time the state-resolved surface reactivity of CH_4 in its totally symmetric CH stretch vibration (ν_1). Comparison of our results with those using direct IR excitation of the ν_3 and $2\nu_3$ vibrations confirms the qualitative predictions of simple vibrational adiabatic calculations and wave packet simulations [7,8] and suggests that quantitative predictions of methane reactivity will require dynamical calculations on a realistic multidimensional potential energy surfaces [28]. Our results clearly indicate that statistical models do not capture the essential physics of the reactive encounter and therefore can neither qualitatively nor quantitatively predict methane chemisorption.

We gratefully acknowledge Professor A. Utz for sharing an updated and extended data set for $S_0(\nu_3)$ on Ni(100) prior to publication, as well as Professor D. Nesbitt for helpful discussions on the adiabatic model.

*Author to whom correspondence should be addressed. Electronic address: rainer.beck@epfl.ch

[1] M. B. Lee, Q. Y. Yang, and S. T. Ceyer, J. Chem. Phys. **87**, 2724 (1987).
[2] P. M. Holmblad, J. Wambach, and I. Chorkendorff, J. Chem. Phys. **102**, 8255 (1995).
[3] A. C. Luntz, J. Chem. Phys. **102**, 8264 (1995).
[4] M. N. Carre and B. Jackson, J. Chem. Phys. **108**, 3722 (1998).
[5] A. L. Utz (private communication).
[6] L. B. F. Juurlink *et al.*, Phys. Rev. Lett. **83**, 868 (1999).
[7] R. Milot and A. P. J. Jansen, Phys. Rev. B **61**, 15 657 (2000).
[8] L. Halonen, S. L. Bernasek, and D. J. Nesbitt, J. Chem. Phys. **115**, 5611 (2001).
[9] M. P. Schmid *et al.*, J. Chem. Phys. **117**, 8603 (2002).
[10] R. D. Beck *et al.*, Science **302**, 98 (2003).
[11] A. Bukoski and I. Harrison, J. Chem. Phys. **118**, 9762 (2003).
[12] H. L. Abbott, A. Bukoski, and I. Harrison, J. Chem. Phys. **121**, 3792 (2004).
[13] Y. Xiang and J. Z. H. Zhang, J. Chem. Phys. **118**, 8954 (2003).
[14] M. P. Schmid *et al.*, Rev. Sci. Instrum. **74**, 4110 (2003).
[15] R. R. Smith *et al.*, Science **304**, 992 (2004).
[16] J. Palma and D. C. Clary, J. Chem. Phys. **115**, 2188 (2001).
[17] J. R. Fair *et al.*, J. Chem. Phys. **116**, 1406 (2002).
[18] S. Yoon *et al.*, J. Chem. Phys. **119**, 9568 (2003).
[19] G. C. Schatz, J. Chem. Phys. **71**, 542 (1979).
[20] G. C. Schatz, M. C. Colton, and J. L. Grant, J. Phys. Chem. **88**, 2971 (1984).
[21] J. C. Corchado, D. G. Truhlar, and J. Espinosa-Garcia, J. Chem. Phys. **112**, 9375 (2000).
[22] J. Palma, J. Echave, and D. C. Clary, Chem. Phys. Lett. **363**, 529 (2002).
[23] S. Yoon *et al.*, J. Chem. Phys. **116**, 10 744 (2002).
[24] H. A. Bechtel *et al.*, J. Chem. Phys. **120**, 5096 (2004).
[25] A. Owyoung, C. W. Patterson, and R. S. Mcdowell, Chem. Phys. Lett. **59**, 156 (1978).
[26] H. A. Bechtel *et al.*, J. Chem. Phys. **120**, 791 (2004).
[27] A. Sinha, J. D. Thoemke, and F. F. Crim, J. Chem. Phys. **96**, 372 (1992).
[28] G. J. Kroes *et al.*, Acc. Chem. Res. **35**, 193 (2002).